Load and Temperature Influence on a GW-SHM System for a Composite Fuselage

Maria Moix-Bonet[1,a *], Daniel Schmidt[1,b], Benjamin Eckstein[2,c] and Peter Wierach[1,d]

[1] German Aerospace Center e.V., Institute of Lightweight Systems, Lilienthalplatz 7, 38108 Braunschweig, Germany

[2] Airbus Operations GmbH, Airbus-Allee 1, 28199 Bremen, Germany

[a] maria.moix-bonet@dlr.de, [b] daniel.schmidt@dlr.de,
[c] benjamin.eckstein@airbus.com, [d] peter.wierach@dlr.de

Keywords: Guided Waves, Environmental and Operational Conditions, Composite Structures, Aeronautic Structures

Abstract. A full-scale composite door surrounding aircraft structure was instrumented with a GW-SHM system and subjected to three representative quasi-static load cases using a hydraulic test rig. The test was performed in a hangar under uncontrolled temperature environment, resulting in broad temperature variations throughout the experiment. This work focuses on differentiating between benign environmental and operational conditions and barely visible impact damage. A data-driven approach based on Gaussian Processes is used to detect barely visible impact damage introduced during the test campaign, differentiating between benign environmental/operational conditions and barely visible impact damage.

Introduction

The design of aircraft structures has evolved over the years, with the introduction of composite materials leading to new requirements for damage tolerance and structural integrity ([1]). The integration of composite materials in aeronautics offers numerous benefits, but also introduces unique challenges related to damage and failure modes. Currently, the safety of composite structures is guaranteed through the use of damage-tolerant designs and traditional non-destructive inspection methods.

Guided Wave-based Structural Health Monitoring (GW-SHM) has emerged as a promising technique for identifying defects in composite aircraft structures. This method employs a network of permanently installed sensors to generate and receive ultrasonic Guided Waves, allowing for the detection of subtle changes in the structure's integrity ([2],[3]). However, one of the primary challenges facing GW-SHM is the impact of environmental and operational conditions on its performance.

Aircraft structures are subject to a wide range of variations in temperature, pressure, and other factors that can affect the propagation of Guided Waves. This can compromise the effectiveness of GW-SHM systems, which often rely on baseline data to detect anomalies. Compensating for these changes remains an active area of research, with numerous techniques having been proposed ([4],[5]). However, applying these methods in real-world scenarios is frequently challenged by the complex geometry of monitored structures and the simultaneous presence of multiple environmental and operational factors. Thus, this study focuses on using a GW-SHM system to monitor damage in a full-scale composite aircraft fuselage under varying load and temperature.

Experimental Setup: An Aircraft Composite Panel

A composite fuselage structure was employed in this study, which is representative of a passenger door region found on wide-body aircraft, such as the Airbus A350. The test structure has dimensions of 4100 mm x 5700 mm and comprises multiple frames, stringers, windows, and a surrounding door structure ([6]).

A custom-designed Guided Wave-based Structural Health Monitoring (GW-SHM) system was integrated onto the fuselage panel. The GW-SHM system's key features include a robust transducer network, reliable transducer connections, and a modular architecture ([7]). This design focuses on sensor reliability and practical application in an industrial setting.

The test rig described in [8] and illustrated in Fig. 1 was used to apply representative loads to the fuselage panel, simulating conditions encountered during flight. Three basic load cases were selected for this study: uniaxial tension, lateral bending left, and vertical bending down. Fig. 1 provides a visual representation of these selected load cases, including their orientation on a barrel level.

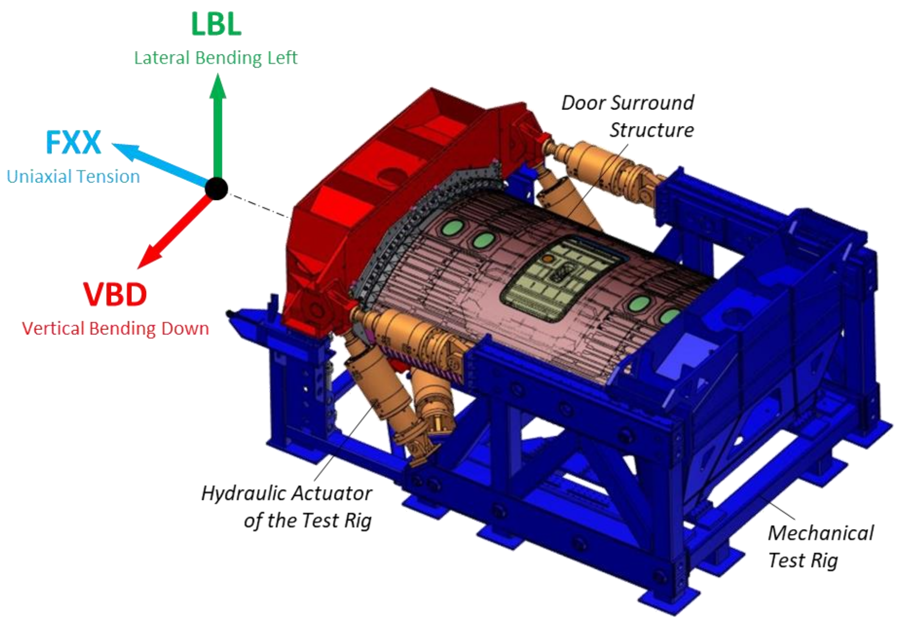

Fig. 1: Composite Fuselage Panel in a Test Rig ([8])

To evaluate the effectiveness of the GW-SHM system, three load cases were applied in a quasi-static manner until a load equivalent to 75% of the structure's Limit Load was reached. The Limit Load (LL) represents the maximum permissible load during normal operation. The quasi-static test paused at multiple steps between the unloaded condition and 75% LL to allow for measurements at various static load levels.

To introduce damage into the fuselage structure, impacts were applied using a gas gun, according the standardized method described in [9]. The impacts created Barely Visible Impact Damage, including delamination and debonding with sizes ranging from 364 mm² to 3720 mm². non-destructive inspection by phased array ultrasonics was performed at the impact locations to gather reference data.

The fuselage structure was equipped with a multi-sensor network, consisting of 148 piezoelectric transducers, 14 strain gauges, and 31 temperature sensors.

Guided Wave-based SHM and changing Environmental and Operational Conditions
There is extensive literature available regarding the sensitivity of GW to environmental and operational conditions and its consequences for the damage identification using GW-SHM systems.

Temperature is a main factor influencing GW propagation, with numerous studies showing its impact on wave velocity and amplitude in composite materials ([10],[11]). Temperature variations affect the response of such SHM systems through multiple mechanisms, including the thermal dependence of the piezoelectric effect, the material properties of the monitored structure and the coupling between transducer and structure.

In contrast to temperature's extensive literature, the behavior of guided waves under stress is less well understood. Changes in phase velocity ([12]) and amplitude ([13]) due to tensile load have been reported in correlation with tensile loads, while [14] observed anisotropic behavior in GW propagation, resulting in increased phase velocity in the direction of tension and decreased phase velocity perpendicular to it. However, research is mostly limited to specific cases involving isotropic materials and uniaxial loading conditions.

The current use case involves a combination of multi-axial loading and temperature variation. To investigate the effects of tensile loading and temperature on GW propagation, the signal response from actuator 1 and sensor 3, which corresponds to a highly loaded area, has been selected. To monitor strain, the measurements of an adjacent strain gauge installed in the actuator-sensor path direction have been used. The maximum strain in this direction during the tensile load case reached 1675$\mu\varepsilon$.

The signal response for an actuation frequency of 70 kHz is plotted at several load levels in Fig. 2(a) and within a temperature range of 12.8°C to 24.2°C in Fig. 2 (right). The signal has been cropped to focus on the main GW-mode propagating at 70kHz: the anti-symmetric (A_0) fundamental mode. In Fig. 2(a), the amplitude increases and the time-of-flight (ToF) decreases as the load is increased. In contrast, Fig. 2(b) shows a decrease in amplitude and an increase in ToF with increasing temperature.

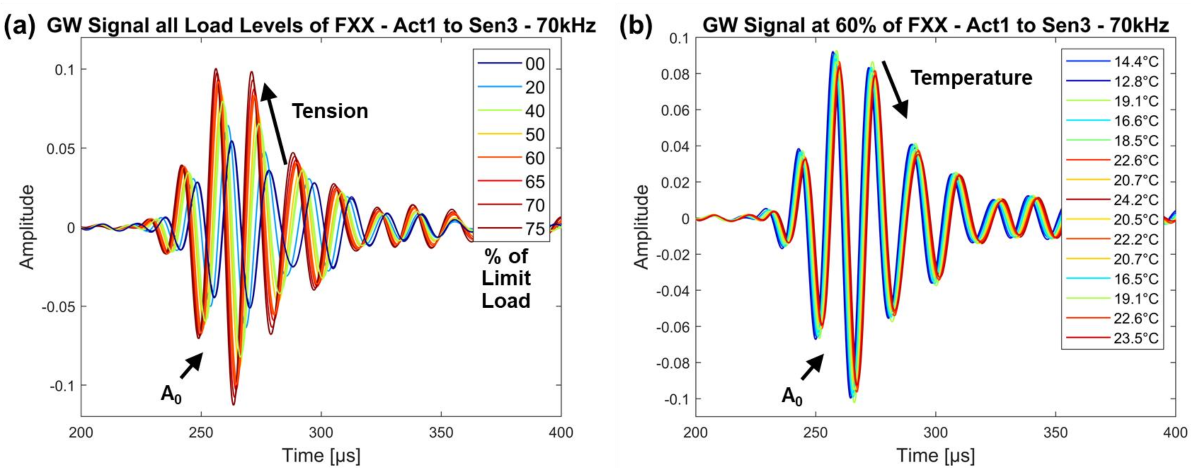

Fig. 2: Guided Wave Signal from Actuator 1 to Sensor 3 – Load (a) and Temperature (b) Effects

To quantify the effects of Environmental and Operational Conditions (EOC), two features have been derived from the GW signal: amplitude and ToF. The amplitude is defined as the maximum amplitude of the Hilbert envelope over the selected wave packet. The reference ToF is calculated using cross-correlation between the actuation pulse and received signal. Subsequent changes in ToF due to load variations are determined through local temporal coherence of the Cross Wavelet Transform, as shown in [15].

Fig. 3 displays all load-temperature combinations acquired during the test campaign in a load level vs. temperature plot. Each point represents the EOC at the time of a GW measurement. The experiment spanned 12 load-unload cycles over six weeks, during which the structure's temperature fluctuated due to the non-climatized environment.

The color range of the scatter plots in Fig. 3 indicates the amplitude and ToF of the GW measurement acquired at each plotted load-temperature combination. For this path, the analysis shows that the dominant effect on the variation of GW-propagation is the load level across both signal features, with a significant increase in amplitude and decrease in ToF.

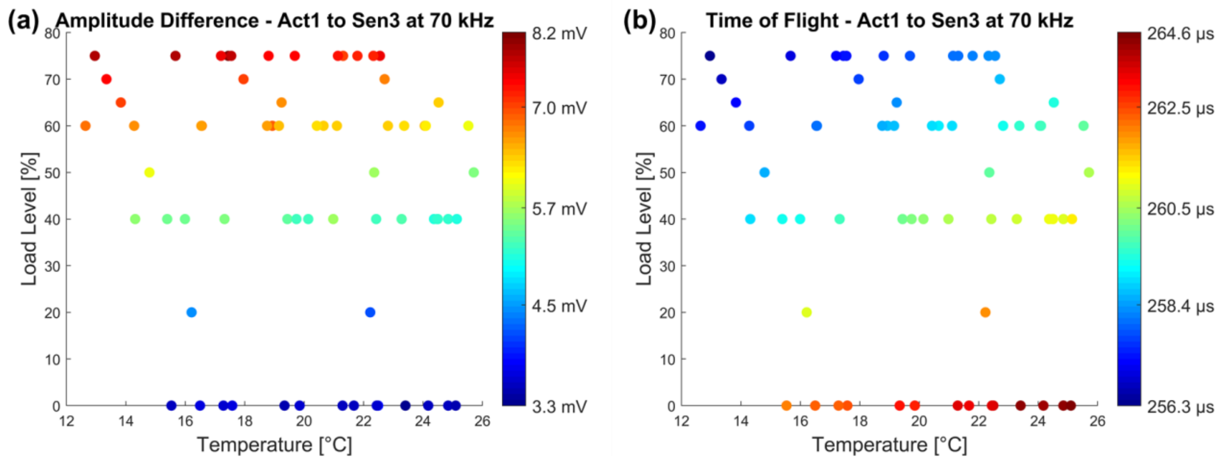

Fig. 3: Amplitude (a) and Time-of-Flight (b) for Temperature and Load Level

It is essential to note that both temperature and load fields are not constant throughout the entire structure, nor do they change uniformly across its geometry. The complex geometry of the structure also means that GW-signals often present interferences, which can lead to non-linear or non-monotonic signal changes in response to temperature and load variations. This is in contrast to the monotonic and even linear relationships between the GW-features and the load and temperature changes observed in Fig. 1 and Fig. 2. A more detailed description of the combined effects of load and temperature during this test campaign can be found in [16].

We now face the challenge of developing a statistical model that can capture the complexity of GW-signals and EOC. Our goal is to identify a model that can distinguish between benign load and temperature effects and damage effects, allowing us to offer reliable SHM capability under such challenging conditions.

Gaussian Process for Damage Detection in changing Environmental and Operational Conditions

Gaussian Processes (GPs) have been increasingly applied in the field of SHM to localize impacts using acoustic emission ([17]), to model of time-series in vibration analysis ([18]) or to quantify damage be means of guided waves ([19]), just to mention a few examples.

For detailed guidance on applying GPs to machine learning tasks, [20] provides an outstanding framework in their work, covering the mathematical formulation of GPs in depth.

This work uses Gaussian Process Regression (GPR) to perform an unsupervised damage detection by means of GW-SHM. For that, GPR is employed to connect a set of input operational variables with the resulting information from the GW-SHM system, using temperature and load as input features and a selected signal feature from the GW-signals as output variable.

The proposed method involves the following key steps:

1. Data Acquisition: Collect GW-data with the monitored structure in its pristine state, under EOC that are representative of the current application scenario. Simultaneously acquire relevant data to the EOC, such as load and temperature.
2. Training a GPR model: Use collected pristine-state data to train a GP model, where load and temperature serve as independent variables and ToF of the GW-data as the dependent variable. The chosen covariance kernel for the GPR model is the squared exponential kernel.
3. Likelihood of new data points: Upon acquiring new GW data and corresponding EOC information in an unknown structural state, apply the fitted GP model for classic anomaly detection. Calculate the likelihood of new data belonging to the pristine state using the GP distribution at specific load-temperature combinations.
4. Damage Detection: Identify potential damage when likelihood exceeds a predefined threshold and covariance uncertainty falls below a predetermined value. If the GP model's uncertainty is too high due to limited information in the region, mark the result as inconclusive.

Some advantages of GPs over other machine learning methods for damage detection with GW-SHM are ([20]):

1. Handling uncertainty: GP models inherently incorporate uncertainty into their predictions, manifesting increased covariance values in feature spaces where data points are scarce or absent. This is particularly useful in monitoring scenarios where data is often noisy and limited.
2. Flexibility: Ability to handle non-linear relationships between inputs and outputs. Complex geometries can lead to interferences in GW-signals, causing non-linear or non-monotonic changes in the signal features in response to temperature and load variations.
3. Scalability: GPs can handle large datasets and high-dimensional feature spaces. GPs can be extended to accommodate multiple input variables, such as complex multi-axial load states as independent variables or high dimensional features to describe GW-signals.

Results

This section aims to understand and assess GPR as a method method to detect damage using a GW-SHM system within the current application scenario: a composite fuselage structure under representative flight loads and temperature variations typical of a non-climatized hangar. For that the GP-based method previously described will be applied exemplarily on an actuator-sensor path affected by introduced impact damage.

The first step involves performing a GPR on the GW-signals acquired from the structure in its pristine state. Fig. 4(a) provides an illustration of how GPR fits to the observed data and demonstrates how data availability affects the GPR fit.

Fig. 4(a) displays the observed time shift values over the two independent variables (load level and temperature) fitted in a GPR model along with the 95% confidence bounds. Three additional views of the fitted GPR model are plotted in Fig. 4: plots (b) to (d). These views visualize the results in two dimensions and highlighting selected data points. Plot (b) shows a 2D cut at 0% load, where numerous GW data points were acquired in pristine condition, resulting in low uncertainty and narrow prediction intervals. In contrast, plot (c) illustrates a 2D cut at 30% load, where uncertainty is higher due to limited available data. Plot (d) presents a 2D cut at 18°C. While temperature is an uncontrolled parameter with randomly scattered data points across its range, the load level is a controlled parameter, resulting in consistent measurements only at predefined loads. This visualization highlights the impact of limited data at certain load levels.

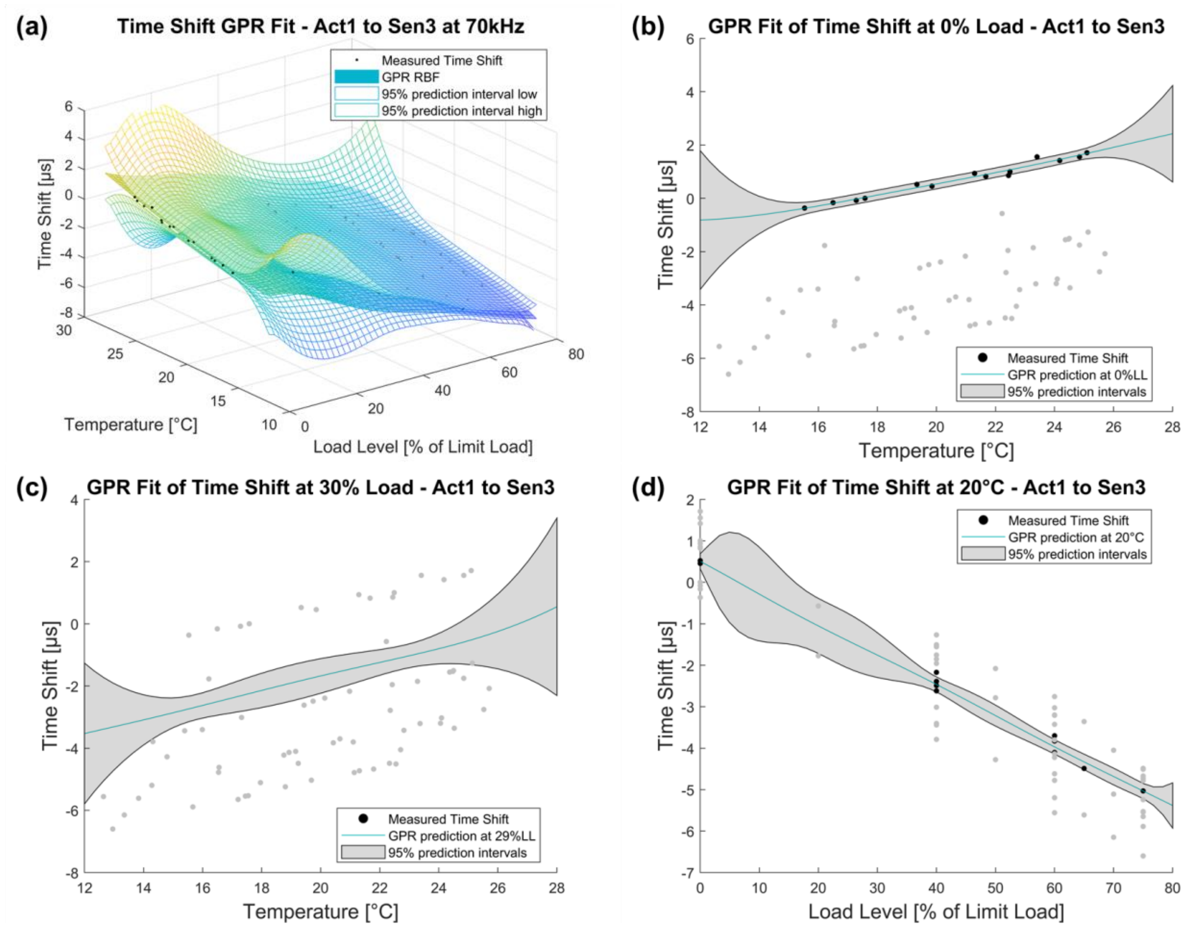

Fig. 4: (a) GPR fit of a single path with load level and temperature as independent variables and time shift as GP-output. 2D cut of GP model at 0% load (b), 30% load (c) and 20°C (d)

To examine the influence of damage combined with load, an actuator-sensor path featuring damage presence have been selected. This particular path was affected by an impact event towards the end of the test campaign, which caused a delamination of approximately 20x29 mm² in size. This visual representation provides an insight into the interaction between operational factors and damage, and how GPs can be used to discriminate between the two.

Fig. 5 presents unsupervised damage detection with a GPR model fitted on GW-data acquired in a pristine state. The GPR fit in 3D, shown in Fig. 4(a), is displayed again but with an alternative actuator-sensor path that runs transversely to the applied load direction. This results in the Guided Waves experiencing compression instead of tension. Thus, the GPR fit shows a monotonic increase in time shift for both higher temperatures and higher load levels.

Fig. 5(b) provides a 2D cut of the 3D GPR fit, representing the model at a constant load level of 0% or unloaded state. The plot distinguishes between points used for training, which are colored in black for those at 0% load and grey for others. The colored points display the observed time shift values acquired during the unsupervised detection phase, where the color scale corresponds to the calculated likelihood or how well the fitted GPR model explains the observed new data.

The two marked data points, acquired after the impact event, clearly deviate from the 95% confidence bounds. One data point falls outside the temperature range used to train the GPR model due to high covariance in the affected area, rendering it difficult to clearly identify the damage. In contrast, the second point is within the temperature and load ranges used for training, and its deviation from the fitted GPR model indicates an anomalous observation.

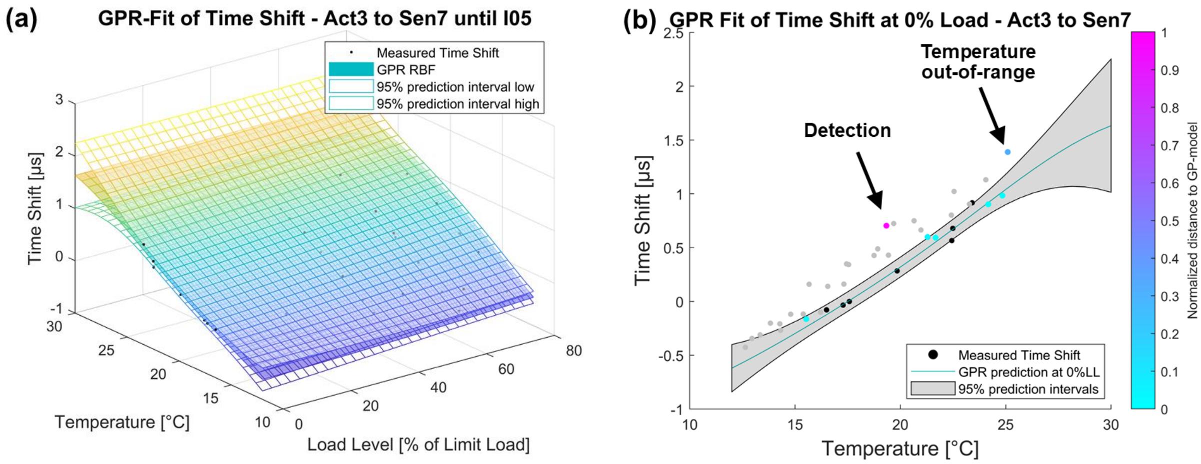

Fig. 5: (a) Gaussian Process Regression fitted on Time Shift for Actuator 3 to Sensor 7 Path (b) GPR fit at 0% Load with Training and Test Data Points

The results show that excluding load information would not allow differentiation between operational conditions and damage, highlighting the importance of considering load effects in the architecture and signal processing design of GW-SHM-systems. The similarity in time shift between these anomalous points and those observed at other load levels (grey points) underscores the importance of accounting for load effects when designing GP models.

Summary

A Guided Wave-based Structural Health Monitoring (GW-SHM) system has been installed on a representative composite fuselage structure. A full-scale test, including multi-axial mechanical loading and the induction of Barely Visible Impact Damage, has generated a comprehensive dataset for the application of GW-SHM in realistic scenarios.

The dataset reveals the effects in GW propagation due to variations in both mechanical loads and temperature. An analysis highlights the relationship between two GW-signal features, time-of-flight (ToF) and amplitude, and the measured environmental and operational conditions.

This dataset has been used to evaluate a novel damage detection algorithm based on Gaussian processes (GP). The approach employs anomaly detection, where GW-data collected in a pristine state are used to train a GP model with load and temperature as input variables and a selected signal feature as output. When new data points arrive, the likelihood of each point belonging to the trained GP model is calculated. The results show that a GP-based detection algorithm is effective in distinguishing between Environmental and Operational Conditions (EOC) and damage for a successful structure monitoring in the presented application scenario.

Acknowledgements

We would like to express our gratitude for the support provided by the Federal Ministry of Economics and Climate Protection (BMWK) through their funding of this project under the LuFo VI framework concept, grant agreement numbers 20D2105G. The success of this research initiative was made possible through the collaborative work with our partners.

References

[1] European Union Aviation Safety Agency. (2018). Easy Access Rules for Large Aeroplanes (CS-25) (Initial issue)

[2] Ricci, F., Monaco, E., Maio, L., Boffa, N. D., & Mal, A. K. (2016). Guided waves in a stiffened composite laminate with a delamination. Structural Health Monitoring, 15(3), 351–358.

[3] Moix-Bonet, M., Eckstein, B., Loendersloot, R., & Wierach, P. (2015). Identification of Barely Visible Impact Damages on a Stiffened Composite Panel with a Probability-based Approach. 10th International Workshop on SHM.

[4] Douglass, A. C. S., & Harley, J. B. (2018). Dynamic Time Warping Temperature Compensation for Guided Wave Structural Health Monitoring. IEEE Transactions on Ultrasonics, Ferroelectrics, and Frequency Control, 65(5), 851–861.

[5] Worden, K., Cross, E. J., Antoniadou, I., & Kyprianou, A. (2014). A multiresolution approach to cointegration for enhanced SHM of structures under varying conditions – An exploratory study. Mechanical Systems and Signal Processing, 47(1–2), 243–262.

[6] Kruse, F., Kühn, M., Krombholz, C., Ucan, H., & Torstrick, S. (2015, September 2). Production of a Full Scale Demonstrator-Structure within the FP7 Project "Maaximus." 5th International Workshops on Aerostructures.

[7] Schmidt, D., Moix-Bonet, M., Galiana, S., & Wierach, P. (2023, September). Integration von angepassten und dezentralen Structural Health Monitoring Systemen in Faserverbundstrukturen. Deutscher Luft- Und Raumfahrtkongress (DLRK).

[8] Sachse, M., Götze, M., Nebel, S., Berssin, S., & Göpel, C. (2020). Testing approach for over wing doors using curved fuselage panel testing technology. Lecture Notes in Mechanical Engineering, 831–837.

[9] Federal Aviation Administration. (2018). Certification and Compliance Considerations for Aircraft Products with Composite Materials.

[10] Lanza di Scalea, F., & Salamone, S. (2008). Temperature effects in ultrasonic Lamb wave structural health monitoring systems. The Journal of the Acoustical Society of America, 124(1), 161–174.

[11] Yinghui Lu, & Michaels, J. E. (2009). Feature Extraction and Sensor Fusion for Ultrasonic Structural Health Monitoring Under Changing Environmental Conditions. IEEE Sensors Journal, 9(11), 1462–1471.

[12] F. Chen, & P.D. Wilcox. (2007). The effect of load on guided wave propagation. Ultrasonics, 47(1–4), 111–122.

[13] Roy, S., Lonkar, K., Janapati, V., & Chang, F.-K. (2014). A novel physics-based temperature compensation model for structural health monitoring using ultrasonic guided waves. Structural Health Monitoring, 13(3), 321–342.

[14] Gandhi, N., Michaels, J. E., & Lee, S. J. (2012). Acoustoelastic Lamb wave propagation in biaxially stressed plates. The Journal of the Acoustical Society of America, 132(3), 1284–1293.

[15] Eckstein, B., Moix-Bonet, M., & Bach, M. (2014). Analysis of Environmental and Operational Condition Effects on Guided Ultrasonic Waves in Stiffened CFRP Structures. 7th European Workshop on SHM

[16] Moix-Bonet, M., Schmidt, D., Eckstein, B., & Wierach, P. (2024). A Composite Fuselage under Mechanical Load: a case study for Guided Wave-based SHM. 11th European Workshop on SHM.

[17] Hensman, J., Mills, R., Pierce, S.G., Worden, K., & Eaton, M. (2010). Locating acoustic emission sources in complex structures using Gaussian processes. Mechanical Systems and Signal Processing, 24(1), 211-223.

[18] Avendaño-Valencia, L. D., Chatzi, E. N., & Tcherniak, D. (2020). Gaussian process models for mitigation of operational variability in the structural health monitoring of wind turbines. Mechanical Systems and Signal Processing, 142, 106686.

[19] Amer, A., & Kopsaftopoulos, F. (2023). Gaussian process regression for active sensing probabilistic structural health monitoring: experimental assessment across multiple damage and loading scenarios. Structural Health Monitoring, 22(2), 1105-1139.

[20] Rasmussen C.E., Williams C.B. (2006) Gaussian processes for machine learning. MIT Press.